

Measured Correlated Motion of Three Massive Coulomb Interacting Particles

L. M. Wiese, O. Yenen, B. Thaden, and D. H. Jaecks

Behlen Laboratory of Physics, University of Nebraska, Lincoln, Nebraska 68588-0111

(Received 11 August 1997)

We have measured the correlated center-of-mass (c.m.) motion and energy sharing of the three massive Coulomb-interacting particles $H^+ + H^+ + H^-$ with total energy of a few eV. We measured in time coincidence the lab frame energy and angle of all three particles produced from excited 4 keV H_3^+ formed in collisions with He. For each triple coincidence, we found the c.m. energy of each particle and the c.m. correlation angle between the two H^+ . The c.m. energy data, displayed on a Dalitz plot, reveals the high degree of correlated motion of the three massive charged particles. [S0031-9007(97)04800-X]

PACS numbers: 34.90.+q

The description of the motion of three bodies, interacting through some potential, with total energy in the continuum, is a classic and fundamental problem of physics. In the case where the three particles interact via long range Coulomb forces, one has the possibility of a high degree of correlated motion in the system because all three particles interact over the entire path of their motion. A full quantal description of such a three-body system must include these long range interaction terms over the entire path of all three particles.

Experimental studies of the continuum three-body problem, in which two of the particles have a charge opposite to the third, have centered around systems that include a massive positive nucleus and two light electrons. Such three-body systems are formed by threshold ionization of atoms by electron impact, as well as double photoionization of negative ions and neutral atoms [1]. In these systems, the energy available to the three particles in the center-of-mass (c.m.) frame is inequitably shared. The fraction of available energy carried away by the ion is limited by momentum conservation to a maximum of $2m_e/M_{\text{ion}}$, and the major part of the available energy is carried away by the two very light electrons. Thus, a determination of the energy and mutual emission angle of the two electrons relative to the essentially stationary nucleus is sufficient to determine the final state dynamics completely. This is not the case if all three particles are of comparable mass, as with $H^+ + H^+ + H^-$, because in the c.m. frame the available energy has the possibility of being more equitably shared among the three particles. For three equal mass particles, momentum conservation limits the fraction of available energy carried away by any one of the three particles to a maximum of $\frac{2}{3}$. To completely ascertain the final state dynamics of the three-body, massive system, a determination of the energy and relative scattering angle of all three particles in the c.m. frame is necessary.

Feagin [2] discussed the theoretical development of the Coulomb three-body problem, beginning with Wannier's classical description of threshold ionization [3], and the subsequent semiclassical redevelopment of Wannier's

theory by Peterkop [4] and Rau [5,6], and the extension of theory to systems of arbitrary mass with total angular momentum $L = 0$ by Klar [7]. Feagin further developed the theory for systems of arbitrary mass and charge and $L > 0$ [2]. Because a complete quantal description or wave function for the Coulomb three-body problem does not exist, the original assumption of Wannier theory has proliferated to all subsequent theoretical developments. The Wannier assumption for near threshold breakup is that, in the reaction zone where the three particles are close together, the system must develop such that the particle of opposite charge becomes located between the two particles of like charge, near the center of charge of the two like-charge particles.

Previous experimental studies of the $H^+ + H^+ + H^-$ system have been limited to the energy distribution of H^- [8,9] and measurement of $H^+ - H^-$ coincident pairs [10,11]. For near threshold breakup of a Coulomb system, Feagin [2] has predicted that the angular distribution between the particles of like charge will be centered at $\phi_{12} = \pi$ with FWHM of 8.06° for $H^+ + H^+ + H^-$. Yenen *et al.* [10] have identified the excited states of H_3^+ that lead to $H^+ + H^+ + H^-$. Gailitis [12] has predicted the partitioning of available energy for two electron emission from a heavy ion, but no prediction exists for the $H^+ + H^+ + H^-$ system.

The only presently viable method of studying the c.m. dynamics of three massive Coulomb-interacting particles is to carry out a three-body half collision experiment in which one studies the dissociation of a fast moving excited molecular ion into the three-body, Coulomb-interacting channel. By colliding 4 keV H_3^+ with a He target gas cell, we produced the excited, fast moving H_3^+ that dissociate into the three-body, Coulomb-interacting system $H^+ + H^+ + H^-$ [8]. We have completely determined in a triple coincidence experiment the final laboratory dynamics of the three-body system $H^+ + H^+ + H^-$. Transforming the results to the c.m. of the dissociating ion, we have determined the correlated c.m. motion of these three equally massive particles. We have measured the total amount of c.m. energy shared among the three

fragments and the c.m. energy of each individual particle, as well as the c.m. angle ϕ_{12} between the two H^+ .

Our experimental approach is illustrated in Fig. 1 by the Newton diagram of the excited, fast moving H_3^+ that dissociates to the experimental final state channel $H^+ + H^+ + H^-$ with total c.m. energy of ε_i . Measurements of the three laboratory kinetic energies $E_i = m_i V_i^2/2$ and scattering angles θ_i of the two H^+ and H^- produced in the dissociation of an excited H_3^+ determine all of the physical parameters in the c.m. system. Specifically, for each triply coincident event of two H^+ and an H^- , we determine the three c.m. energies ε_i and c.m. scattering angle ϕ_{12} between the two H^+ , as well as the deflection angle α and the inelastic energy loss Q of the H_3^+ in its collision with the He target. The index $i = 1, 2$ refers to H^+ , while $i = 3$ refers to the H^- .

From the Newton diagram and conservation of energy and momentum, the c.m. energy ε_i of each particle is

$$\varepsilon_i = \frac{1}{9} \left[(4E_i + E_j + E_k) - 4\sqrt{E_i E_j} \cos(\theta_i - \theta_j) - 4\sqrt{E_i E_k} \cos(\theta_i - \theta_k) + 2\sqrt{E_j E_k} \cos(\theta_j - \theta_k) \right], \quad (1)$$

from which the total available c.m. energy ε_i to be shared among the three particles is found. The c.m. correlation angle ϕ_{12} between the two H^+ is related to the c.m. energies by

$$\cos(\phi_{12}) = \frac{1}{2} \left(\frac{\varepsilon_3}{\sqrt{\varepsilon_1 \varepsilon_2}} - \sqrt{\frac{\varepsilon_1}{\varepsilon_2}} - \sqrt{\frac{\varepsilon_2}{\varepsilon_1}} \right). \quad (2)$$

For $H_3^+ \rightarrow H^+ + H^+ + H^-$, the observed c.m. energies of the fragments are in the few eV range. Because energy is proportional to velocity squared, the energies observed in the laboratory frame extend over a much larger range. As a result, the error on the measured c.m. energy, determined from the measured laboratory energies, undergoes a compression when making a Galilean transformation from the laboratory frame to the c.m. frame [13].

The electrostatic energy analyzer that measures all three laboratory energies and angles in a triple coincidence experiment has been described in a previous publication

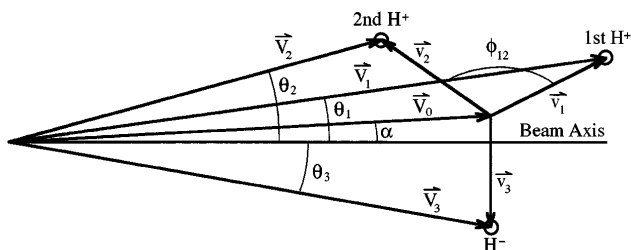


FIG. 1. Newton diagram for the dissociation of H_3^+ into $H^+ + H^+ + H^-$. V_0 is the velocity of the c.m. of the dissociating H_3^+ and α is the H_3^+ deflection angle. $V_i(v_i)$ is the velocity of the i th particle in the laboratory (c.m.) frame. θ_i is the laboratory scattering angle of the i th particle and ϕ_{12} is the c.m. angle between the two H^+ . The size of the v_i 's relative to the V_i 's is greatly exaggerated for clarity.

[14]. Each of the three fragments is collected by its own position sensitive detector, utilizing two 40 mm active area microchannel plates along with a wedge-and-strip anode. Each detector provides two Cartesian coordinates, used to determine the laboratory angle and energy of the fragment, and a fast timing pulse from the microchannel plates. Since the three measured laboratory energies result from particles coming from the same excited parent H_3^+ , the transformed c.m. energies are insensitive to the energy spread of the primary 4 keV H_3^+ ion beam or to the width (0.76 mm) of the ion beam.

The three position sensitive detectors sample a limited range of c.m. energy sharing configurations, but can be repositioned to cover a wide range of c.m. energy sharing configurations. We positioned the detectors to measure the near collinear breakup of H_3^+ along the beam direction. The positioning of the H^+ detectors limited one of the H^+ to c.m. scattering forward, or near 0° with respect to the H_3^+ beam direction, while the other was scattered backward, or near 180° . The forward moving H^+ is designated as the first H^+ , while the H^+ moving backward is designated as the second H^+ (see Fig. 1). The detection system accepted H_3^+ breakups with c.m. angle between the H^+ of $170 \leq \phi_{12} < 210^\circ$.

The three fast timing pulses are used to measure the arrival time differences T_{12} , T_{31} , and T_{32} between each pair of fragments for each triply coincident event. A histogram of the timing data is shown in Fig. 2. The background of the timing spectrum has four components. An overall constant background forms due to three uncorrelated particles arriving at the detectors within the timing limits of the coincidence electronics. The other three components arise from coincidences among two correlated and one uncorrelated fragment, and appear as ridges, or walls, in the timing spectrum. The ridge formed

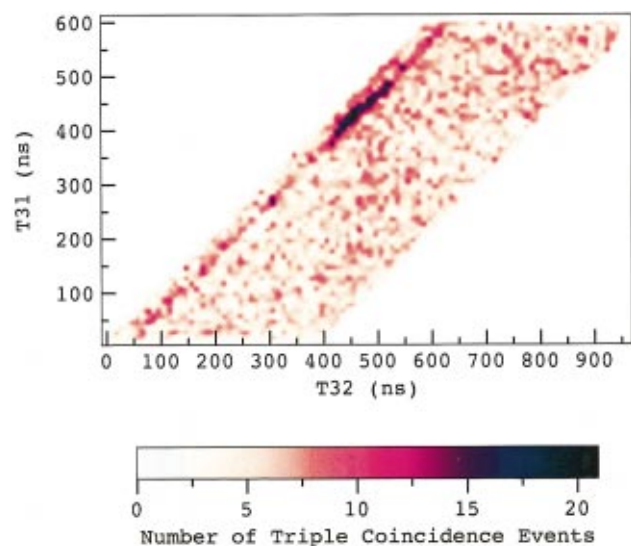


FIG. 2(color). Timing spectrum for $H^+ + H^+ + H^-$ triple coincident events. T_{31} is the time-of-flight difference between the H^- and the first H^+ ; T_{32} is the time-of-flight difference between H^- and the second H^+ .

by the triple coincidence of two correlated H^+ and an uncorrelated H^- can be seen running diagonally on the left edge of the timing spectrum. Coincidences from a correlated H^+-H^- pair and an uncorrelated second H^+ form faint, broad horizontal and vertical bands. The overlap of the three ridges form a background triple coincidence peak in the spectrum, and the real triple coincidence peak forms on top of it. Subtracting the background from the triple coincidence timing spectrum in Fig. 2, we find a real triple coincident peak of 251 ± 27 events. Acquisition time for this spectrum was 750 h. The rate for real triple events was 0.9×10^{-4} Hz.

For each triple event, we measure the laboratory energy and scattering angle of each of the three fragments. Equations (1)–(3) are used to transform the three energies and scattering angles from laboratory coordinates to c.m. coordinates. The events that lie in the region of the real triple coincidence peak are approximately $\frac{3}{5}$ background and $\frac{2}{5}$ real triple events. Because the background triple events contain at least one uncorrelated particle, typically the set of measured laboratory quantities ($E_1, E_2, E_3, \theta_1, \theta_2, \theta_3$) or, equivalently, the transformed set of c.m. quantities ($\varepsilon_1, \varepsilon_2, \varepsilon_3, \phi_{12}, Q, \alpha$), for background triple events is unphysical. Subsequently, most of the background events can be identified and separated from the events that form the real triple coincidence peak. For example, the inelastic energy loss Q calculated for the triple coincidence event may be negative, indicating a superelastic scattering of the H_3^+ in its collision with the He target. Because the H_3^+ must absorb energy during the collision to be promoted to an excited state, the collision must be inelastic, not superelastic.

To graphically accentuate three-body correlations, we use a triangular Dalitz plot [15], shown in Fig. 3. For an arbitrary three-body system of masses m_1, m_2 , and m_3 we use the set of reduced c.m. energy coordinates $m_i \varepsilon_i / R$, where

$$R \equiv m_1 \varepsilon_1 + m_2 \varepsilon_2 + m_3 \varepsilon_3. \quad (3)$$

For nonrelativistic speeds, the coordinate $m_i \varepsilon_i / R$ is the ratio of p_i^2 to $p_i^2 + p_2^2 + p_3^2$. On the Dalitz plot, each of the reduced c.m. energy coordinates is plotted as the perpendicular distance from one of the sides of the equilateral triangle. Because of our choice of normalized coordinates, the height of the triangle is unity. For any point inside the triangle, the sum of the three coordinates is equal to one, satisfying energy conservation requirements. Events that satisfy momentum conservation, for nonrelativistic systems, will lie inside the inscribed circle in Fig. 3 [16]. The purpose of using reduced coordinates is that, for any combination of three arbitrary masses, the momentum conservation limit will always be the inscribed circle in Fig. 3. For the three-body system $H^+ + H^+ + H^-$, all masses are equal, and the reduced c.m. energy coordinates become $\varepsilon_i / \varepsilon_t$, the fraction of total c.m. energy carried away by each particle.

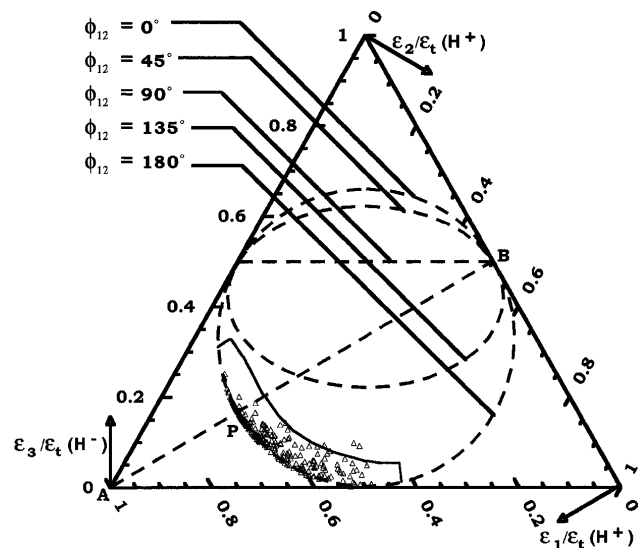


FIG. 3. Dalitz plot of the sharing of available energy among the three particles. The fraction of energy carried away by the H^- , $\varepsilon_3/\varepsilon_t$, is plotted as the vertical distance from the base of the triangle. The H^+ energy fractions, $\varepsilon_1/\varepsilon_t$ and $\varepsilon_2/\varepsilon_t$, are plotted as the perpendicular distance from the other two sides of the triangle. The approximate range of energy sharing configurations probed by the present setup is indicated by the solid curve. Energy sharing configurations in which momentum is conserved are located inside the circle. Lines of constant ϕ_{12} , the c.m. angle between the two H^+ , are also shown.

If, for the process producing the three-body system, the energy sharing among the three particles is determined solely by phase space considerations, the resulting triple coincidence events will produce a uniform distribution on a Dalitz plot. Any deviation from a uniform distribution indicates a noncontact interaction among the three particles. A long range Coulomb interaction or an electron exchange interaction inside the reaction zone, could affect the energy sharing by enhancing some configurations, while depleting others, causing a clumping of events on a Dalitz plot.

The real triple coincidence events, shown on the Dalitz plot in Fig. 3, illustrate how the energy is shared among the fragments in a three-body system. Total c.m. energies were 4 to 14 eV, with 70% of all events in the range of $5 < \varepsilon_t < 8$ eV. For each event, ε_t is known to within 0.5%. The fraction of energy carried away by the H^- is plotted as the vertical distance from the base of the triangle. The H^+ energy fractions are plotted as the perpendicular distance from the other two sides of the triangle. The approximate range of energy sharing configurations probed by the present setup is indicated by the solid curve. The circle itself corresponds to the collinear breakup, with the lower two-thirds of the circle corresponding to configurations in which the c.m. angle ϕ_{12} between the two H^+ is 180° , and the upper third corresponding to $\phi_{12} = 0^\circ$. Lines of constant ϕ_{12} are also shown for $\phi_{12} = 45^\circ, 90^\circ$, and 135° . Line AB extending from the lower left corner corresponds to

configurations in which the H^- and the second H^+ have matching energies. Above line AB , $\varepsilon_3 > \varepsilon_2$, and below line AB , $\varepsilon_3 < \varepsilon_2$.

The intersection of line AB and the circle at point P correspond to configurations in which the H^- and second H^+ escape together, with matched c.m. energy and scattering angle. It is here on the Dalitz plot that we observe a dense band of events along the momentum conservation limit where $\phi_{12} = 180^\circ$. Figure 4 shows an expanded view of the Dalitz plot data in Fig. 3, emphasizing the detailed structure of the data and density of events. Bracket I marks the extent of the dense band of events at point P . The density of these events is indicative of the high degree of correlation.

The final system $H^+ + H^+ + H^-$ can be formed through an intermediate doubly excited state of H_2 ,



and the triple coincidence events from this two-body breakup would form a band as seen in Fig. 4. The location of the band along line AB is determined by the amount of energy liberated in the breakup of the H_2^{**} relative to that liberated in the H_3^+ two-body fragmentation. The fact that the band lies right on the momentum conservation limit indicates little or no energy available to the $H^+ - H^-$ pair to share from the breakup of the H_2^{**} . Treating the system as the result of this two-body breakup and using momentum conservation, we can determine the total energy available to the $H^+ - H_2^{**}$ pair in the fragmentation of the $(H_3^+)^*$, as well as the energy available to the $H^+ - H^-$ pair in the breakup of the H_2^{**} . For the dense band of events at point P in Fig. 4, the energy the $H^+ - H^-$ pair has to share is less than 0.1 eV for all events and typically ≤ 0.01 eV. The small relative energy indicates that the H_2^{**} only formed very near the threshold for producing a $H^+ - H^-$ ion pair.

In the absence of postcollision effects, the breakup of the H_2^{**} would occur along an arbitrary orientation, producing a symmetric band of events about line AB . As can be seen in Fig. 4, the intense band of events is not symmetric. Configurations in which the H^- has less c.m. energy than the second H^+ are more likely. This indicates a preference in the three-body system for configurations in which the H^- lies between the two H^+ , suggesting a quasi-two-body breakup in which the H^- and second H^+ , by virtue of their proximity to each other, appear to be bound, but are still influenced by the first H^+ .

Another feature of the real triple coincidence data, indicated by bracket II in Fig. 4, is the collection of events near the base of the Dalitz plot. For these events, the two H^+ share most of the available energy, while the H^- gets a small share, typically $< 10\%$, and always lies between the two H^+ . Unlike the events that form the band at point P in Fig. 4, the events near the base of the Dalitz plot are not confined to the strict collinear configuration. The departure of these events from the collinear configuration

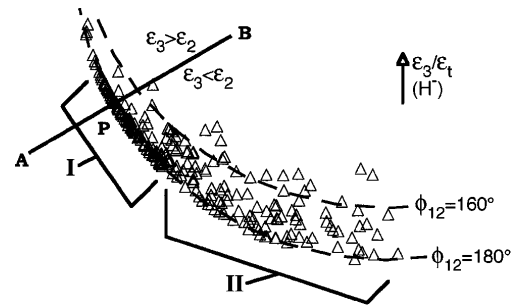


FIG. 4. Dalitz plot of data in Fig. 3, expanded to emphasize the high degree of correlation. Line AB and point P are identical to that in Fig. 3. Bracket I marks a dense band of events at point P . These events collect only in the collinear configuration for which $\phi_{12} = 180^\circ$, and correspond to the quasi-two-body breakup of H_3^+ . The events indicated by bracket II depart from the collinear configuration.

is illustrated in Fig. 4 by the lines of constant ϕ_{12} for $\phi_{12} = 160^\circ$ and 180° .

In conclusion, we have observed for the first time triple coincidences for the near collinear breakup of H_3^+ into the Coulomb-interacting channel of $H^+ + H^+ + H^-$ and determined the c.m. dynamics of each triple coincidence event completely. A Dalitz plot of the sharing of available c.m. energy among the three fragments indicates a tendency for the H^- to escape with one of the H^+ , yet remain between the two H^+ .

This work is supported by the National Science Foundation under Grant No. PHY-9419505.

- [1] S. Jones and D.H. Madison, in *The Physics of Electronic and Atomic Collisions*, Proceedings of the XIX International Conference, edited by Louis J. Dubè, J. Brian A. Mitchell, J. William McConkey, and Chris E. Brion, AIP Conf. Proc. No. 360 (AIP, New York, 1995), p. 341; A. Huetz *et al.*, *ibid.*, p. 139.
- [2] J. M. Feagin, *J. Phys. B* **17**, 2433 (1984); **30**, 693 (1997).
- [3] G. H. Wannier, *Phys. Rev.* **90**, 817 (1953).
- [4] R. Peterkop, *J. Phys. B* **4**, 513 (1971).
- [5] A. R. P. Rau, *Phys. Rev. A* **4**, 207 (1971).
- [6] A. R. P. Rau, *J. Phys. B* **9**, L283 (1976).
- [7] H. Klar, *Z. Phys. A* **307**, 75 (1982).
- [8] O. Yenen, D. H. Jaecks, and L. M. Wiese, *Phys. Rev. A* **39**, 1767 (1989).
- [9] H. Martinez and A. Amaya-Tapia, *Chem. Phys.* **211**, 299 (1996).
- [10] O. Yenen, D. Calabrese, L. M. Wiese, and D. H. Jaecks, *Phys. Rev. A* **47**, 1059 (1993).
- [11] I. Domiguez *et al.*, *Phys. Rev. A* **50**, 3856 (1994).
- [12] M. Gailitis, *J. Phys. B* **19**, L697 (1986).
- [13] S. M. Trujillo, R. H. Neynaber, and E. W. Rothe, *Rev. Sci. Instrum.* **37**, 1655 (1966).
- [14] D. Calabrese, O. Yenen, L. M. Wiese, and D. H. Jaecks, *Rev. Sci. Instrum.* **65**, 116 (1994).
- [15] R. H. Dalitz, *Philos. Mag.* **44**, 1068 (1953).
- [16] R. Hagedorn, *Relativistic Kinematics* (Benjamin, New York, 1963), p. 101.